

Electrostatics and the Lab on a Chip

T. B. Jones

University of Rochester

Rochester, NY 14625 (USA)

Email: jones@ece.rochester.edu

Abstract

At the heart of the laboratory on a chip are chemical or biochemical probes designed to detect specific molecules or reaction products. For these probes to perform their function, a microfluidic "plumbing system" is needed to accept samples, then manipulate, dispense, and distribute tiny liquid volumes on the chip. The most promising mechanisms for handling such small quantities of liquid -- from microliters down to tens of picoliters -- are all electrostatic, e.g., electrocapillarity, electroconvection, electrophoresis, electro-osmosis, and dielectrophoresis. Despite years of study of these effects, the body of existing work is an imperfect guide to their effective exploitation in microfluidic applications. Attempts to harness electrostatic forces in structures <100 microns in size often encounter unanticipated behavior. Such surprises can be attributed to dramatic changes in the relative influences of the various competitive forces (e.g., viscous shear, surface wetting, and capillarity). In this paper, some of the more promising avenues of research on electric-field-mediated microfluidics are examined. To explicate why and when electrostatic forces can be advantageous in the lab on a chip, Trimmer's bracket notation is invoked to perform an investigation of the scaling laws for microfluidic systems. The methodology facilitates examination of the effects of device size on throughput, processing time, temperature rise, and other important measures of system performance.

1. Introduction

Micro total analysis system (μ TAS) technology [1] seeks to replace the conventional tools of chemists, biological scientists, and medical researchers with programmable, robotic microsystems capable of performing rapid chemical/biochemical analyses or protocols using very small inventories of liquid analyte and reagent. Such systems -- intended to replace conventional test tubes, well plates, cell culture dishes, capillaries, as well as liquid chromatographs, cell cytometers and other cumbersome diagnostic instruments -- exemplify the *laboratory on a chip*. This revolutionary concept promises massive parallelism plus sufficient improvements in automation and speed to eliminate or greatly ameliorate serious bottlenecks in conventionally equipped laboratories that stem from the unavoidable need to perform large numbers of experiments to satisfy the requirements of statistical significance of data.

Applications for the laboratory on a chip range widely, from microreactors for the chemical industry and pharmacological screening systems for drug discovery, to microbiological diagnostic machines and genetic research tools. In combinatorial chemistry, the ability to conduct large numbers of reactions under closely controlled conditions automatically and simultaneously using very small analyte and reagent volumes is understandably attractive. The use of small liquid inventories (microliters or less) will significantly reduce mixing and reaction times, to say nothing of cost. Furthermore, being able to operate with small quantities is attractive in biomedical research where, quite often, only very small inventories of rare cells or substances can be isolated and made available for testing. Another benefit of these robotic microsystems is that, with minimal need for human intervention, experiments and tests involving dangerous chemicals and pathogens can be conducted more safely.

Key sub-systems of the laboratory on a chip include a user interface, sensors, (bio)chemical probes, and some sort of *microfluidic system*. The last of these, the microfluidic system, is the "plumbing infrastructure" essential for the manipulation, dispensing, and transport of liquids around the chip. A variety of surface and volume force mechanisms are under consideration to achieve precision fluid control, including capillarity [2], surface wetting [3], electro-osmosis [4], electroconvection [5], electrowetting [6], and liquid dielectrophoresis (DEP) [7]. One interesting hybrid μ TAS concept would use microfluidics to transport and dispense liquid aliquots that themselves contain suspended bioparticles (cells, DNA, etc.). After dispensing small volumes of the particle-bearing liquid at pre-determined sites on a chip, the DEP force exerted on individual

particles within each droplet would be used to probe the particles, sorting and differentiating them according to requirements of the process [8]. The subject of this paper is the electrostatic forces available for *particle* and *liquid* manipulation in the laboratory on a chip.

2. Electrostatic force scaling for microsystems

During the early years of the VLSI circuit technology revolution, Richard Feynman was already anticipating MEMS (microelectromechanical systems) and μ TAS technology. Such remarkable prescience was no doubt based on a recognition that the laws of physics do not exhibit symmetry with respect to changing physical dimensions [9], in other words, that the relative magnitudes of forces are rearranged when size is changed. One consequence of these “rearrangements” crucial to MEMS and μ TAS is that electrostatic forces become increasingly important as devices become smaller. William Trimmer recognized the broad significance of force scaling in engineered microsystems and devised a bracket notation, which he used for systematic investigations of their scaling laws. He was able to show just how electrostatic forces effectively dominate over magnetic forces in MEMS devices [10]. In this paper, we employ an approach based on Trimmer’s methods to explore the scaling advantages of electrostatic forces for the laboratory on a chip using two examples: DEP manipulation of particles and electric-field-mediated microfluidics.

3. Scaling laws for particle DEP

Dielectrophoresis, the force exerted by a nonuniform electric field on uncharged, dielectric particles [11], either attracts particles to regions of strong electric fields or repels them, depending on their polarizability relative to the medium in which they are dispersed. See Fig. 1. Without loss of generality from the standpoint of scaling, we restrict attention here to spherical particles of radius R and relative dielectric constant ϵ_p in a fluid medium with ϵ_m . The DEP force may be expressed as a series of multipolar contributions, including dipolar, quadrupolar, and higher-order terms [12].

$$\bar{F}_{\text{DEP}} = 2 \epsilon_0 \left[\frac{K_1 R^3}{3} \bar{E} \cdot \bar{E} + \frac{K_2 R^5}{30} \bar{E} : \bar{E} + \dots \right] \quad (1)$$

where $K_n = n(2n+1)(\epsilon_p - \epsilon_m)/[(n+1)\epsilon_m + n\epsilon_p]$ is a polarization coefficient and ϵ_0 is the permittivity of free space.

The need for a systematic investigation of the scaling rules for DEP is evident from the observation that the dipolar term depends on R^3 while the quadrupolar term is proportional to R^5 . First, we define scale factors for the important parameters: ℓ for the electrode dimensions, R for the particle radius, and V for voltage. Then, for example, the electric field E and the del operator scale as ℓ^{-1} and ℓ^{-1} , respectively. Adopting Trimmer’s bracket notation [10], the scaling laws for the two leading terms in \bar{F}_{DEP} are:

$$\left[\bar{F}_{\text{DEP}} \right] = \begin{array}{cc} -3 & 3 & 2 & \text{dipoleterm} \\ -5 & 5 & 2 & \text{quadrupoleterm} \end{array} \quad (2)$$

In this notation, brackets enclosing an algebraic term on the lhs of an equation represent the operation of extracting the scaling factors of the term. Subscripts identify any constraints imposed. On the rhs in brackets are the scale factor “values”. When convenient, a matrix-like format with columns and rows is used to tabulate different force laws and/or physical constraints. For example, on the rhs of Eq. (2), the upper row is reserved for the dipole force term and the lower row is for the quadrupole; to keep track of more multipolar terms, one simply adds more rows. The value of the

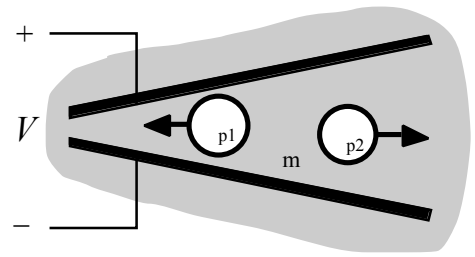


Fig. 1. Dielectrophoretic (DEP) attraction (or repulsion) of particles depends on the relative values of particle & suspending liquid dielectric constants. Here, $\epsilon_{p1} > \epsilon_m$ and $\epsilon_{p2} < \epsilon_m$.

bracket notation for MEMS systems is realized when force laws are combined with various constraints to gain insights into the effect of reducing physical dimensions, as exemplified below.

3.1 Particle levitation and trapping

The DEP force offers a gentle, controllable means to levitate or to trap particles suspended in aqueous media using easily

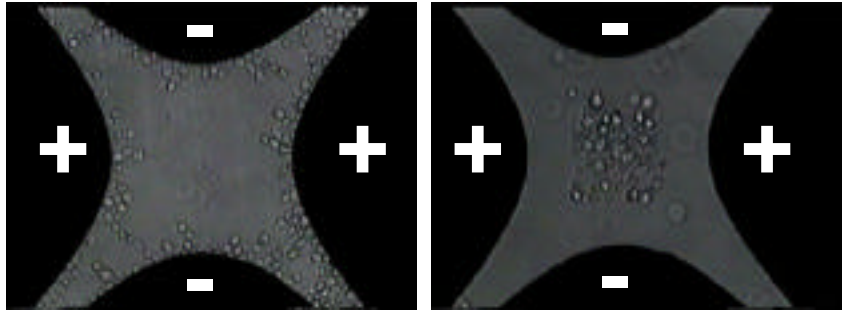


Fig. 2. Planar quadrupole particle trap. At the left, particles exhibit +DEP and thus collect at field maxima. At the right, particles exhibit -DEP, forming a loose ensemble near the center where the field magnitude goes to zero. (these photos courtesy of P. Gascoyne, Univ. of Texas at Houston)

fabricated microelectrodes. For example, Fig. 2 depicts a planar quadrupolar trap for + and -DEP.

Static force balance for a particle levitated or trapped against the gravitational force is:

$$\bar{F}_{\text{DEP}} + 4 (\rho_p - \rho_m) R^3 \bar{g} / 3 = 0 \quad (3)$$

where ρ_p and ρ_m are particle and liquid medium densities, respectively, and \bar{g} is the gravitational acceleration vector. Consider adjusting the scale factors while maintaining the particle at a fixed, that is, a geometrically similar position within the structure. One can analyze this situation by performing the previously introduced bracket operation on Eq. (3) and equating the terms.

$$\text{dipole only : } = \frac{3}{2} \frac{1}{2}; \text{ quadrupole only : } = \frac{5}{2} \frac{1}{2} \quad (4)$$

These relations, one each for dipolar and quadrupolar structures, readily reveal one advantage of reducing the size of DEP levitation structures. Keeping particle size fixed ($\rho = 1$) while reducing all electrode dimensions by a factor of 2 (i.e., $\rho = 1/2$), reduces the levitation voltage by a factor of $2^{3/2}$

2.83 for dipolar electrodes, and by $2^{5/2}$ 5.66 for quadrupolar structures. On the other hand, keeping the electrodes fixed ($\rho = 1$) while reducing particle size by the factor of 2 (i.e., $\rho = 1/2$) leaves levitation voltage *unchanged* for dipolar structures, but *increases* it by a factor of 2 for quadrupolar structures. Eq. (5) summarizes these voltage-scaling rules for fixed particle size, and also includes scaling rules for electric field E and temperature rise due to Joule heating T for these particle traps. Refer to the Appendix for a short synopsis of the scaling law governing temperature.

V		dipolar	quadrupolar	
\bar{E}		3/2	5/2	
T	levitation against gravity fixed particle size	1/2	3/2	=
		3	5	

(5)

It is to be recognized that scaling rules do not provide all the information necessary to decide between dipolar and quadrupolar levitators for a given application; nevertheless, the exercise does facilitate useful comparisons between the two electrode structures. Of these two types of particle traps, quadrupolar electrodes seem to have clear advantages with respect to voltage requirements, maximum electric field, and heating as size is reduced. These advantages are not fully realized in the control of biological cells using electrode structures in the 10 to 100 micron size range, but could become very valuable in nanostructures under development for analysis and manipulation of DNA and other nanoscale proteins and particles.

3.2 Particle dynamics

Most applications for particulate DEP in the lab on a chip will quite likely involve dynamic behavior. Thus, one critical dynamic performance measure is the response time t , e.g., the time

required to achieve some targeted level of particle separation or concentration, or the residence time required in a flow-through analyzer. To investigate, we start with the equation of motion for the particle. On the micron scale, momentum is negligible and the drag force dominates. If Stokes' drag can be used, the equation of motion takes a simple form.

$$\bar{F}_{\text{DEP}} - 6 \mu_m R \bar{v} = 0 \quad (6)$$

where μ_m is the dynamic viscosity of the liquid and \bar{v} is particle velocity. Let the scaling factor for all time variables be t . Assume that the dipole force dominates, and perform the bracket operation on Eq. (6) subject to the fixed particle size condition. Two physical constraints are considered: fixed velocity v (i.e., $v^{-1} = 1$) and fixed response time t (i.e., $t = 1$). Of these two, fixed response time seems a more relevant performance measure for the lab on a chip.

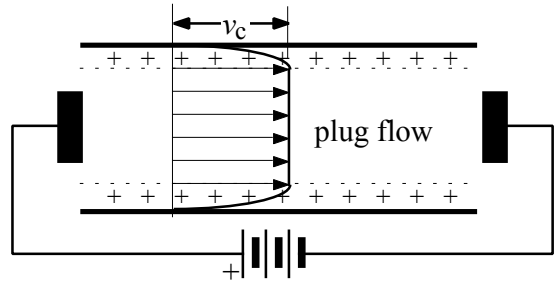


Fig. 3. Basic description of DC electro-osmotic effect in a channel. The tangential electric field imposed by external DC voltage exerts a force on the free ions in the double-layer adjacent to the walls. The resulting shear force pumps the liquid.

V		=	fixed velocity	fixed response time	(7)
\bar{E}			3 / 2	2	
T			1 / 2		
	dipole force only		3	4	
	Stokes drag				
			fixed particle size		

Eq. (7) reveals to us that decreasing structure size while keeping the response time t fixed (i.e., $t = 1$) achieves significant benefits in reducing voltage requirements, electric field magnitude, and operating temperature.

4. Scaling laws for E-field-mediated microfluidics

Most electric-field-mediated microfluidic schemes can be categorized as electrochemical and/or electrohydrodynamic (EHD) in nature. Yet, despite the authoritative works of Levich [13], Melcher [14], Taylor [15], and others, surprises await those attempting to harness electrical forces to actuate liquids in <100 micron sized structures. These surprises stem from the unfamiliar ways that well-known phenomena combine on the microfluidic scale. The two cases considered here are electro-osmotic flow and electrowetting/DEP actuation.

4.1 Electro-osmotic flow

Ions in a liquid electrolyte close to a metal wall are subject to strong diffusion effects that separate the + and - species. This selective process creates a thin sheath called the Helmholtz double-layer adjacent to the boundary. In this layer, ions of one sign predominate. A tangential DC electric field E_{tan} imposed along the length of the channel acts on the ions in this layer and creates a pumping force. Electro-osmosis shows promise as a controllable microfluidic pumping scheme, and Levich's formula [13, pp 474-475] may be used to assess its utility in microsystems.

$$\bar{v}_c = - \frac{\zeta}{\mu_m} \bar{E}_{\text{tan}} \quad (8)$$

where ζ is the zeta potential and $|\bar{v}_c|$ is the essentially flat velocity for plug flow in the channel center. Refer to Fig. 3. Scaling Eq. (8) yields the relationship $v_c^2 = \zeta^2 E_{\text{tan}}^2 / \mu_m^2$. The volume flow of liquid W scales as $W \propto v_c^2 \propto \zeta^2 E_{\text{tan}}^2 / \mu_m^2$. Subject to the condition that the microchannel dimensions remain large compared to the thickness of the Helmholtz layer, scaling laws for the important performance parameters of an electro-osmotic pump may be obtained.

$$\begin{array}{c}
 V \\
 \bar{E} \\
 T \\
 W \\
 t
 \end{array}
 \left|
 \begin{array}{c}
 \text{fixed } W \\
 \text{fixed } t \\
 \\
 \\
 \text{fixed double-} \\
 \text{layer thickness}
 \end{array}
 \right.
 =
 \begin{array}{cc}
 \begin{array}{cc}
 \text{fixed } W & \text{fixed } t \\
 -1 & 2 \\
 -2 & \\
 -2 & 4 \\
 1 & 3 \\
 3 & 1
 \end{array}
 & (9)
 \end{array}$$

It is quite evident from Eq. (9) that fixing volume flow while simultaneously reducing structure size leads to excessive voltages, electric field magnitudes, and operating temperature values. On the other hand, these same quantities are reduced if the response time is fixed as size is decreased.

4.2 Static electrowetting and DEP actuation

Electrowetting using dielectric-coated electrodes (EWOD) and DEP liquid actuation are, respectively, the low- and high-frequency manifestations of the electrostatic force exerted by a non-uniform electric field on polarizable media [16]. Figs. 4 and 5 show EWOD and DEP actuation structures. Because these mechanisms are capable of rapid manipulation and movement of relatively large liquid volumes, they are receiving considerable attention for use in the lab on a chip. In this and the next section, respectively, we investigate static liquid orientation against gravity and the dynamic transient response of a liquid. These phenomena are chosen to be representative models for EWOD and DEP applications in a microfluidic system.

Consider the vertical, parallel-plate geometry of Fig. 6. The structure on the left uses a conductive liquid and electrodes coated with an insulator of thickness d and dielectric constant ϵ_d , while that on the right uses insulating liquid and bare electrodes. Limiting expressions for static height-of-rise h as defined in Fig. 6 are:

$$h = \begin{cases} \epsilon_d \epsilon_0 V^2 / 4 D d (1 - \epsilon_u) g, & \text{EWOD, low frequency} \\ (\epsilon_d - \epsilon_u) \epsilon_0 V^2 / 2 D^2 (1 - \epsilon_u) g, & \text{DEP, high frequency} \end{cases} \quad (10)$$

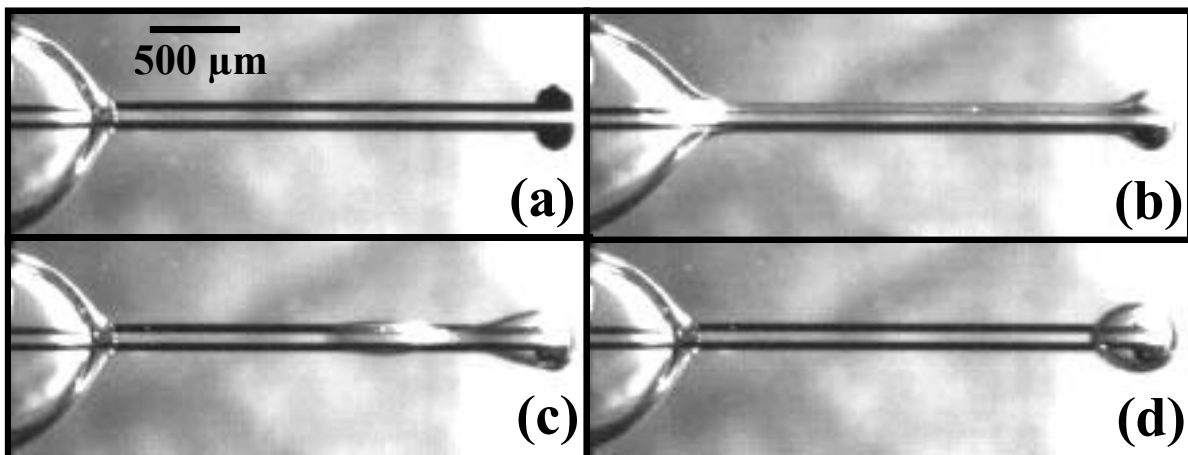


Fig. 5. DEP actuation of water using co-planar electrodes patterned on a substrate and coated with a dielectric layer (a). Applying AC voltage for ~100 msec, a finger of liquid forms and moves rapidly from left to right (b). When finger reaches the circular electrodes at right, voltage is removed (c) and capillary instability pinches off a droplet (d).

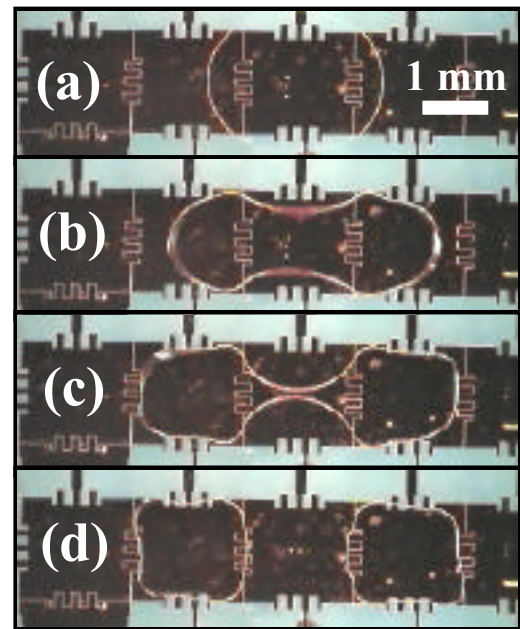


Fig. 4. Splitting of ~200 nanoliter water volume into two equal portions using the electrowetting (EWOD) effect. In the sequence of micrographs shown, the individually addressed, dielectric-coated electrodes are viewed from above through a transparent upper electrode spaced ~100 microns from the lower electrodes. (these photos courtesy of C-J Kim, UCLA)

where the subscripts “u” and “l” refer to properties of the upper and lower liquids, respectively. In the analysis to follow, it is convenient to distinguish d and H from the other electrode dimensions with new scaling factors and T , respectively. Performing the bracket operation on the expressions in Eq. (10), the result is a set of scaling rules for the fixed height-of-rise constraint, (i.e., $h = H$).

$$\left. \begin{array}{l} V \\ \bar{E} \\ T \end{array} \right|_{\text{fixed } H} = \begin{array}{c|cc} & \text{EWOD} & \text{DEP} \\ \hline & 1/2 & 1/2 \\ & 1/2 & -1/2 \\ & \text{NA} & 2 \end{array} \quad (11)$$

Note that for EWOD, the electric field $E = V/2d$ in the insulating dielectric layer and zero in the conductive liquid. Thus, there is virtually no Joule heating. Under the fixed height stipulation, EWOD does not scale as advantageously as DEP, though the constant height constraint is probably not realistic in a practical situation.

4.3 Dynamic electrowetting and DEP actuation

Probably more relevant as a performance measure for application in the lab on a chip than the hydrostatic relationship of h to V is the transient behavior. Of specific interest is the time required for the liquid to rise to the top of the structure when the voltage is turned on suddenly. For the purposes of the scaling analysis, we employ a simple laminar flow model for the fluid mechanics.

$$2wh(t) \mu \frac{v_z}{x} + w D T^e = 0 \quad (12)$$

where the fluid velocity $v_z = dh/dt$ and T^e is the normal electric stress. Gravity may be ignored, but surface wetting hysteresis, also ignored here, may be important.

$$T^e = \begin{cases} \epsilon_0 V^2 / 4Dd, & \text{EWOD, low frequency} \\ \epsilon_0 (1 - \epsilon_u) V^2 / 2D^2, & \text{DEP, high frequency} \end{cases} \quad (13)$$

Combining Eqs. (12) and (13) and then performing the bracket operation, we obtain:

$$\left. \begin{array}{l} V \\ \bar{E} \\ T \end{array} \right|_{\text{fixed response time}} = \begin{array}{c|cc} & \text{EWOD} & \text{DEP} \\ \hline & 1/2 & 1/2 \\ & 1/2 & -1/2 \\ & \text{NA} & 2 \end{array} \quad (14)$$

which is identical to Eq. (11). Again, EWOD actuation has fewer advantages as electrode structures are scaled down. In particular, reducing the dielectric thickness d provides no benefit at all.

5. Conclusion

Any laboratory on a chip based on wet chemical probes requires a plumbing system to dispense and manipulate analyte and reagent liquids. The most promising schemes for achieving this liquid control exploit electrostatic fields. Similarly, electrostatics can be used for precise, controllable

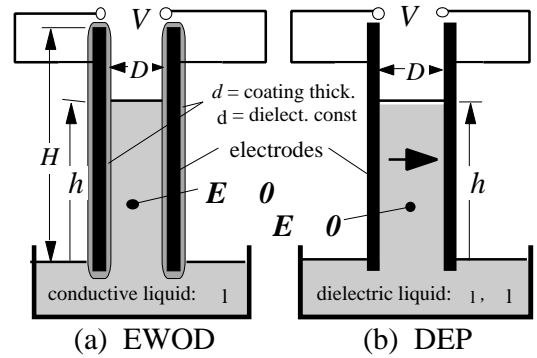


Fig. 6. A basic geometry useful in formulating scaling laws for microfluidic applications of electrowetting-on-dielectric (EWOD) and the dielectrophoretic (DEP) actuation. (a) EWOD electrodes are coated with a very thin dielectric layer, $d \ll D$, and operated at low frequency. At high frequencies, the influence of any coating becomes negligible and the height of rise phenomenon becomes identical to the DEP height-of-rise experiment depicted at the right. (b) DEP electrodes require no dielectric layer if the liquid is sufficiently insulative. The transient response of this geometry when voltage is applied suddenly serves as an adequate model for the dynamic response of a microfluidic device for the laboratory on a chip.

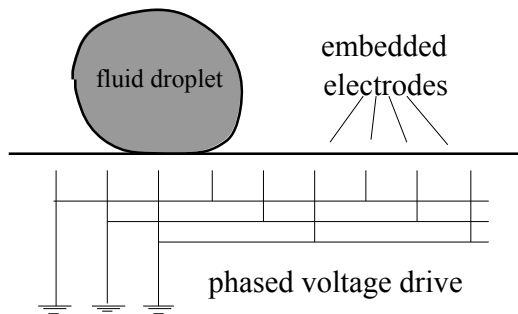
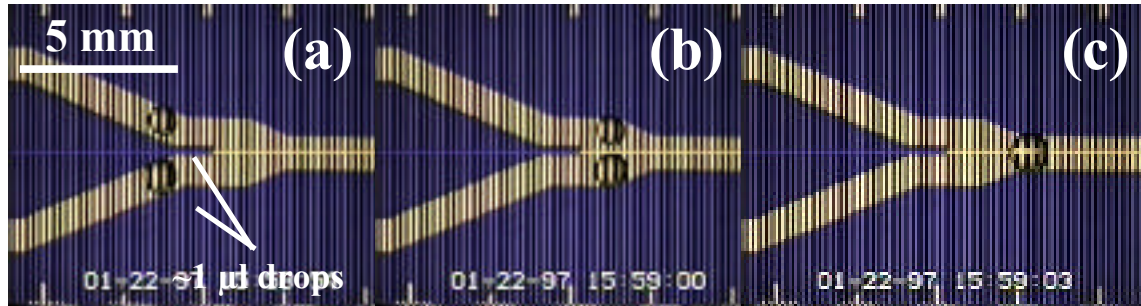


Fig. 7. The electrostatic droplet transport system shown at left consists of parallel electrodes arranged like railroad ties, embedded in a substrate and coated with a dielectric layer. Voltage is applied to the electrodes in sequence causing conductive water droplets to move in response to an electrostatic attractive force. In the micrograph sequence shown below (a), the electrode pitch is $\sim 200 \mu\text{m}$. A pair of $1 \mu\text{l}$ droplets is transported from left to right (b); they coalesce at the junction of the two transport structures just to the right of center (c). (photos courtesy of M. Washizu, Tokyo University, Japan)



conveyance, separation, and collection of particles in liquid suspension. The scaling analyses summarized in this paper reveal unique opportunities for electrostatic forces in microfluidic systems. It is interesting to note that scaling arguments do not require analytical or numerical solution of boundary value problems or initial value transients. Only the governing equations are needed; the scaling relations can be extracted without solving these equations. The value of scaling arguments lies in the ease with which one can identify classes of force effects and sets of physical constraints that yield either (i) significant advantage as size is scaled down or (ii) insurmountable difficulties (e.g., higher required electric fields, excessive operating temperature, etc.). A good example is provided by DEP liquid actuation. Early experiments used electrode structures with millimeter dimensions and voltages exceeding 10 kV [17]. In these structures, actuation of even deionized (DI) water would have been impossible due to excessive Joule heating. However, when the electrode structure size is reduced by a factor of 20, i.e., $\lambda = 1/20$, the scaling rules for both static and dynamic DEP actuation, Eqs. (11) and (14), predict that temperature rise T is reduced by a factor of 400! This prediction is borne out convincingly by experiments reported with DI water in 10 to 100 micron structures [7]. Furthermore, consistent with the scaling prediction for voltage V (i.e., $\lambda = 1/20$), the actuation voltage drops down to 200 to 500 V. Fig. 7 shows another example: an electrostatic droplet transport system that would never work with electrodes on the scale of millimeters. Other examples of how reducing electrode structure size favors electrostatic forces abound and, as a result, research laboratories world-wide are vigorously investigating electric-field-mediated microfluidic systems for the laboratory on a chip.

Acknowledgment

W. S. Trimmer offered the author encouragement to investigate the scaling laws for μTAS technology. E. Cummings, P. Gascoyne, C-J. Kim, T. Schnelle, and M. Washizu graciously provided videos showing examples of electric-field-mediated particle manipulation and microfluidic systems. The author gratefully acknowledges the Japan Society for the Promotion of Science, the US National Science Foundation, the US National Institutes of Health, the Center for Future Health (University of Rochester), and the Infotonics Technology Center, Inc., for their support.

Appendix

Joule heating is a serious problem in many electric-field-mediated microfluidic systems. It can lead to unacceptable increases in temperature and therefore must be considered in microsystem scaling studies. The relationship relating temperature T to Joule heating is:

$$k_m \nabla^2 T - \rho_m c_m \frac{\partial T}{\partial t} = - \rho_m E^2 \quad (A1)$$

where k_m and ρ_m are thermal and electrical conductivities, respectively, ρ_m is mass density, and c_m is specific heat. For the worst-case analysis needed here, the time-dependent term ($\partial T / \partial t$) may be ignored, because the maximum temperature rise occurs in steady-state conditions. Let β be the scale factor for temperature. Then, assuming that overall structure dimensions scale with the electrodes, the scaling operation performed on Eq. (A1) gives $[\nabla^2 T] = \beta^2 = \rho_m E^2$. This result is used directly to establish the scaling laws for T in Eqs. (5), (7), (9), (11) and (14).

References

- [1] See for example the proceedings of the 2002 MicroTAS Conference: Micro Total Analysis Systems 2002, vols. 1 & 2, (Dordrecht, NL: Kluver).
- [2] Harrison DJ, Fluri K, Fan Z, and Seiler K 1995, in Micro Total Analysis Systems 1995, A. Van Den Berg and P. Bergveld, eds. (Dordrecht, NL: Kluver), 105-115; Kataoka DE and Troian SM 1999 *Nature* **402**, 794-797.
- [3] Gau H, S. Herminghaus S, Lenz P, and Lipowsky R 1999 *Science* **283**, 46-49.
- [4] Duffy DC, Schueller OJ, Brittain OJA, and Whitesides GM 1999 *J. Micromech. Microeng.* **9**, 211-217.
- [5] McBride SE, Moroney RM, and Chiang W 1998, in Micro Total Analysis Systems 98, D. J. Harrison and A. Van Den Berg, eds. (Dordrecht, NL: Kluver) 45-48.
- [6] Sondag-Huethorst JAM and Fokkink LGL 1994 *J. Electroanal. Chem.* **367** 49-57; Pollack MG, Fair RB, Shenderov AD 2000 *Applied Physics. Lett.* **77**, 1725-1726; Lee J, Moon H, Fowler J, Schoellhammer T, and Kim C-J 2002 *Sensors Actuators A* **95**, 259-268.
- [7] Jones TB, Gunji M, Washizu M, and Feldman MJ 2001 *J. Applied Physics* **89**, 1441-1448; Jones TB 2001 *J. Electrostatics* **51-52**, 290-299.
- [8] Fuhr G and Shirley SG 1995 *J. Micromech. Microeng.* **5**, 77-85; Hughes MP and Morgan H 1998 *J. Phys. D: Appl. Phys.* **31**, 2205-2210; Gascoyne PRC, Vykoukal J, Weinstein R, Gandini A, and Sawh R, in Micro Total Analysis Systems 2002, vol. 1, (Dordrecht, NL: Kluver), 323-325; Voldman J, Toner M, Gray ML, and Schmidt MA 2002 *J. Electrostatics* **57**, 69-90; Sano H, Kabata H, Kurosawa O, and Washizu M 2002, in Technical Digest (IEEE), 15th Int'l Conf. on Microelectromechanical Systems, 11-14; Cummings EB and Singh AK 2000 Proc. SPIE Conf on Micromachining and Microfabrication **4177**, 164-173.
- [9] Feynman R 1965 *The Character of Physical Law* (Cambridge, MA (USA): MIT Press) 95-96.
- [10] Trimmer WSN 1989 *Sensors Actuators* **19**, 267-287.
- [11] Pohl HA 1951 *J. Applied Phys.* **22**, 869-871.
- [12] Washizu M and Jones TB 1994 *J. Electrostatics* **33**, 187-198.
- [13] Levich VG 1962 *Physicochemical Hydrodynamics* (Englewood Cliffs, NJ (USA): Prentice-Hall).
- [14] Melcher JR 1963 *Field-Coupled Surface Waves* (Cambridge, MA (USA): MIT Press).
- [15] Melcher JR and Taylor GI 1969 *Annual Rev. Fluid Mech.* **1**, 111-146.
- [16] Jones TB 2002 *Langmuir* **18**, 4437-4443.
- [17] Jones TB, Perry MP, and Melcher JR 1971 *Science* **174**, 1232-1233; Jones TB and Melcher JR 1973 *Phys. Fluids* **16**, 393-400.